



# Latency of Spread: An Important Clinical Indicator Reflecting the Complexity Level of Offending Vessels in Patients with Typical Hemifacial Spasm

Xiangyu WEI, Bowen CHANG, Shiting LI

Xinhua Hospital Affiliated to Shanghai Jiaotong University School of Medicine, Department of Neurosurgery, Shanghai, China

Xiangyu Wei and Bowen Chang contributed equally to this work and should be considered co-first authors.

Corresponding author: Shiting LI ✉ lishiting@xinhumed.com.cn

## ABSTRACT

**AIM:** To investigate whether the latency of spread could reflect the complexity level of intraoperative offending vessels in patients with typical hemifacial spasm.

**MATERIAL and METHODS:** A total of 96 patients with typical hemifacial spasm who underwent microvascular decompression (MVD) in our department between August 2018 and December 2019 were retrospectively analyzed. We introduced a new concept of three complexity levels of offending vessels based on six vascular classifications proposed by Kwan Park et al. and the difficulty of intraoperative management reviewed by surgical videos. One-way analysis of variance, Spearman correlation analysis, and multivariate linear regression analysis were performed.

**RESULTS:** There were significant differences in latency of spread among the three complexity levels of offending vessels ( $p < 0.01$ ). Spearman correlation analysis showed a strong negative correlation between vascular complexity level and the latency of spread ( $r = -0.7997$ ,  $p < 0.0001$ ). Multivariate linear regression analysis showed that the vascular complexity level was the main factor affecting the latency of spread ( $p < 0.01$ ). In contrast, other factors such as sex, side, age, hypertension, and diabetes had no significant effects.

**CONCLUSION:** The latency of spread, as an important clinical indicator, can reflect the complexity level of offending vessels in patients with typical hemifacial spasm before MVD.

**KEYWORDS:** Latency of spread, Typical hemifacial spasm, Microvascular decompression, Offending vessels, Complexity level

**ABBREVIATIONS:** HFS: Hemifacial spasm, AMR: Abnormal muscle response, REZ: Root exit zone, MVD: Microvascular decompression, AICA: Anterior inferior cerebellar artery, PICA: Posterior inferior cerebellar artery, VA: Vertebral artery, CSF: Cerebrospinal fluid, MRI: Magnetic resonance imaging, ANOVA: Analysis of variance, NVC: Neurovascular complex

## INTRODUCTION

Hemifacial spasm (HFS) is characterized by involuntary, unilateral, tonic, and/or clonic contractions of the facial musculature. The diagnosis of HFS can be confirmed by its semiology and electrophysiological examination of abnormal muscle response (AMR) (2, 11, 16, 18, 20). The primary

cause is the high neuro-excitability due to the compression of offending vessels at the root exit zone (REZ) of the facial nerve. The current standard treatment is microvascular decompression (MVD), in which the responsible vessels are separated from the facial nerve with Teflon felt (12, 22, 25). Most patients presented with typical symptoms, which initially involve the orbicularis oculi muscle and then gradually spread

downward to the cheek and the orbicularis oris (3,7,10,13). The latency of spread of patients with typical HFS refers to the time interval between the onset of orbicularis oculi muscle and the involvement of lower facial muscles. The latency of spread varies among typical patients (5). In some patients, symptoms may develop rapidly within months, while symptoms may be confined to the orbicularis oculi muscles for years in other cases. To the best of our knowledge, no literature has analyzed the association between latency of spread and offending vessels in patients with typical HFS.

## ■ MATERIAL and METHODS

This study was approved by the Ethic Committee of Xin Hua Hospital Affiliated to Shanghai Jiao Tong University School of Medicine; Approval No: XHEC-C-2020-057; Date: October 27, 2020.

### Patients

We retrospectively reviewed the medical records of HFS patients who received MVD from a single surgeon (S.T.L.) between August 2018 and December 2019 in our department. Patients meeting the following criteria were excluded from this study: 1. Secondary HFS confirmed by imaging examination; 2. Atypical HFS; 3. Inability to recall the latency of spread; 4. No MVD during hospitalization; and 5. Prior MVD surgery was performed in other hospitals.

### Surgical Procedures

Under general anesthesia, each patient was put in a lateral decubitus position and the head was fixed in a frame. The stimulating and recording electrodes were set up for real-time intraoperatively electrophysiological monitoring. A 6-cm-long retro auricular straight incision with 2 cm above and 4 cm below the mastoid was made within the hairline. A craniectomy about 2.5 cm in diameter was obtained far lateral to the sigmoid sinus. A curved dura incision towards the sigmoid sinus was made and sutured back. The arachnoid layer on the lateral side of the cerebellum was opened sharply. Dissection started from the caudal cranial nerves rostrally. With thorough drainage of cerebrospinal fluid (CSF), the flocculus was raised and the entire intracranial course of the facial nerve was explored (1,4,8). Offending vessels should be carefully identified and ZLR used if AMR was unavailable or unstable, or multiple responsible vessels existed. Named after the authors, Dr. Zheng and Dr. Li, ZLR was recorded from the facial muscles when the culprit artery wall was electrically stimulated (18,21,24,26). The appropriate Teflon felt was moved using a micro dissector to separate the conflicting vessels from the facial nerve. The entire surgical procedure should be performed under electrophysical monitoring.

### Compression Types and Complexity Level

Kwan Park et al. classified the compression patterns of offending vessels into six types, namely loop, arachnoid, perforator, branch, sandwich, and tandem type. Loop type is the simplest responsible vessel type, that is, a single vessel compresses REZ of the facial nerve. The arachnoid type involves the thick arachnoid belt, which promotes a closer

contact between the culprit vessels and the facial nerve. The perforating arteries from conflicting vessels in perforator type make the neurovascular complex more cohesive. Branch type means the facial nerve is caught in between the compressing vessel and its branch. When the facial nerve is clamped by multiple vessels, it is a sandwich type. The tandem type means that one vessel compresses another vessel which, in turn, compresses the facial nerve (9,15).

We used this classification in the study. In addition, according to the compressive patterns and the difficulty of intraoperative management reviewed by surgical videos, we have proposed a new concept of the complexity level of offending vessels. Level 1 indicates the condition of responsible vessels is simple and easy to deal with during surgery, while level 3 indicates that the condition of offending vessels is complex and challenging to deal with. Level 2 is between levels 1 and 3.

### Statistical Analysis

Spearman correlation analysis between vascular complexity level and the latency of spread was performed by Graphpad Prism Version 8.0 software. One-way analysis of variance (ANOVA) and multivariate linear regression analysis were performed using SPSS Version 23.0 software. Sex, side, age, hypertension, diabetes, and complexity level were taken as independent variables and the latency of spread was the dependent variable. The p-value < 0.05 was considered statistically significant. The r-value > 0.5 or < - 0.5 was considered a strong correlation.

## ■ RESULTS

A total of 96 patients with typical HFS were included in this study (Table I). There were 33 men and 63 women, with a mean age of  $54.47 \pm 9.86$  years (range 29-75). The left-to-right side ratio was 44: 52. The average duration of symptoms was  $57.97 \pm 51.95$  months (range 6-240), and the mean latency of spread was  $31.92 \pm 25.30$  months (range 3-96). As shown in Table II, the vascular complexity levels were classified into level 1 (n=29), level 2 (n=33), and level 3 (n=34). Level 1 referred only to loop type while level 3 included all the tandem types involving vertebral artery. The mixed types indicated the presence of multiple vascular patterns. Five other cases with mixed types (No.11, 31, 35, 48, and 64) were also defined as level 3. The remaining types belonged to level 2. Samples of different types of responsible vessels were shown in Figure 1A-J. The average latency of spread in complexity levels 1, 2, and 3 were  $62.83 \pm 16.00$  months,  $24.61 \pm 15.02$  months, and  $12.65 \pm 11.42$  months, respectively. Moreover, there were significant differences in latency of spread among these three levels ( $p < 0.01$ ).

Spearman correlation analysis (Figure 2) showed a strong negative correlation between vascular complexity level and the latency of spread ( $r = -0.7997$ ,  $p < 0.0001$ ), indicating that the more complex the offending vessels, the faster the disease may progress from orbicularis oculi muscle down to the lower facial muscles. Moreover, the shorter the latency of spread, the more complex the management of intracranial conflicting vessels. To exclude the effects of sex, side, age,

**Table I:** Baseline Characteristics and Intraoperative Findings of the 96 Patients

| Patients | Sex | Side | Age (years) | Duration (months) | Latency of spread (months) | Hypertension | Diabetes | Offending Vessels | Compression type      | Complexity level |
|----------|-----|------|-------------|-------------------|----------------------------|--------------|----------|-------------------|-----------------------|------------------|
| 1        | F   | R    | 36          | 24                | 18                         | /            | /        | AICA              | Perforator            | 2                |
| 2        | M   | L    | 50          | 12                | 6                          | √            | /        | VA+AICA           | Tandem                | 3                |
| 3        | F   | L    | 70          | 36                | 24                         | /            | √        | AICA+PICA         | Tandem                | 2                |
| 4        | F   | R    | 50          | 24                | 19                         | /            | /        | AICA              | Tandem                | 2                |
| 5        | F   | L    | 65          | 60                | 57                         | √            | /        | AICA              | Branch                | 2                |
| 6        | F   | L    | 59          | 120               | 84                         | /            | /        | AICA              | Loop                  | 1                |
| 7        | M   | L    | 43          | 36                | 12                         | √            | /        | VA+AICA           | Tandem                | 3                |
| 8        | F   | L    | 48          | 48                | 36                         | /            | /        | AICA              | Loop                  | 1                |
| 9        | F   | R    | 48          | 36                | 24                         | /            | /        | AICA              | Branch                | 2                |
| 10       | M   | L    | 58          | 24                | 12                         | /            | √        | VA+AICA           | Tandem                | 3                |
| 11       | F   | R    | 47          | 60                | 24                         | √            | /        | AICA              | Arachnoid, Perforator | 3                |
| 12       | F   | R    | 50          | 12                | 11                         | /            | /        | AICA              | Tandem                | 2                |
| 13       | F   | R    | 42          | 8                 | 6                          | /            | /        | VA+AICA           | Tandem                | 3                |
| 14       | F   | L    | 53          | 36                | 12                         | /            | /        | VA+AICA+PICA      | Tandem                | 3                |
| 15       | F   | L    | 75          | 18                | 5                          | √            | /        | VA+AICA           | Tandem                | 3                |
| 16       | F   | R    | 46          | 120               | 60                         | √            | /        | AICA              | Loop                  | 1                |
| 17       | M   | L    | 72          | 36                | 30                         | /            | /        | AICA              | Loop                  | 1                |
| 18       | M   | R    | 43          | 36                | 12                         | /            | /        | PICA              | Perforator            | 2                |
| 19       | F   | R    | 43          | 36                | 12                         | /            | /        | AICA              | Branch                | 2                |
| 20       | F   | R    | 49          | 36                | 24                         | /            | /        | AICA              | Tandem                | 2                |
| 21       | M   | R    | 43          | 120               | 48                         | /            | √        | AICA              | Tandem                | 2                |
| 22       | F   | R    | 55          | 108               | 60                         | /            | /        | AICA              | Loop                  | 1                |
| 23       | F   | R    | 56          | 96                | 72                         | /            | /        | AICA              | Loop                  | 1                |
| 24       | F   | R    | 66          | 24                | 12                         | √            | √        | VA+AICA           | Tandem                | 3                |
| 25       | M   | R    | 62          | 180               | 60                         | /            | /        | AICA              | Arachnoid             | 2                |
| 26       | M   | L    | 57          | 120               | 48                         | √            | /        | AICA              | Tandem                | 2                |
| 27       | F   | R    | 65          | 108               | 84                         | √            | /        | AICA              | Loop                  | 1                |
| 28       | F   | R    | 57          | 36                | 24                         | /            | /        | AICA              | Perforator            | 2                |
| 29       | F   | L    | 51          | 18                | 15                         | /            | /        | AICA              | Branch                | 2                |
| 30       | F   | R    | 54          | 120               | 60                         | /            | /        | AICA              | Loop                  | 1                |
| 31       | F   | L    | 64          | 12                | 10                         | √            | /        | AICA              | Branch, Arachnoid     | 3                |
| 32       | F   | R    | 52          | 144               | 24                         | √            | /        | AICA              | Perforator            | 2                |
| 33       | F   | R    | 68          | 7                 | 6                          | /            | √        | VA+PICA           | Tandem                | 3                |
| 34       | M   | L    | 67          | 60                | 36                         | /            | /        | VA+AICA           | Tandem                | 3                |
| 35       | F   | R    | 50          | 24                | 12                         | /            | /        | AICA              | Branch, Sandwich      | 3                |
| 36       | F   | R    | 40          | 84                | 60                         | /            | /        | AICA              | Branch                | 2                |
| 37       | F   | L    | 29          | 18                | 12                         | /            | /        | VA+AICA           | Tandem                | 3                |
| 38       | F   | R    | 59          | 12                | 7                          | /            | √        | VA+AICA           | Tandem                | 3                |
| 39       | M   | L    | 36          | 60                | 36                         | /            | /        | VA+AICA           | Tandem                | 3                |
| 40       | F   | R    | 51          | 60                | 36                         | /            | /        | AICA              | Perforator            | 2                |
| 41       | F   | L    | 64          | 120               | 60                         | /            | /        | VA+AICA           | Tandem                | 3                |
| 42       | F   | R    | 62          | 12                | 7                          | /            | /        | VA+AICA           | Tandem                | 3                |
| 43       | F   | R    | 49          | 84                | 24                         | /            | /        | AICA              | Arachnoid             | 2                |
| 44       | M   | L    | 53          | 20                | 10                         | /            | /        | VA+AICA           | Tandem                | 3                |
| 45       | F   | L    | 49          | 24                | 12                         | /            | /        | VA+AICA           | Tandem                | 3                |
| 46       | F   | R    | 59          | 60                | 36                         | /            | /        | AICA              | Sandwich              | 2                |
| 47       | M   | L    | 72          | 12                | 8                          | √            | √        | VA+AICA           | Tandem                | 3                |
| 48       | M   | R    | 44          | 11                | 7                          | /            | /        | AICA              | Branch, Arachnoid     | 3                |
| 49       | F   | R    | 60          | 24                | 18                         | √            | /        | AICA              | Sandwich              | 2                |
| 50       | F   | L    | 52          | 36                | 30                         | /            | /        | AICA              | Arachnoid             | 2                |
| 51       | F   | R    | 66          | 72                | 48                         | /            | √        | AICA              | Loop                  | 1                |

Table I: Cont.

| Patients | Sex | Side | Age (years) | Duration (months) | Latency of spread (months) | Hypertension | Diabetes | Offending Vessels | Compression type  | Complexity level |
|----------|-----|------|-------------|-------------------|----------------------------|--------------|----------|-------------------|-------------------|------------------|
| 52       | F   | L    | 39          | 60                | 12                         | /            | /        | VA+AICA           | Tandem            | 3                |
| 53       | M   | L    | 67          | 120               | 72                         | /            | /        | AICA              | Loop              | 1                |
| 54       | M   | R    | 63          | 66                | 42                         | /            | /        | AICA              | Loop              | 1                |
| 55       | M   | L    | 54          | 12                | 8                          | /            | /        | VA+AICA           | Tandem            | 3                |
| 56       | F   | R    | 67          | 84                | 60                         | √            | /        | PICA              | Loop              | 1                |
| 57       | M   | L    | 71          | 36                | 18                         | /            | /        | AICA+PICA         | Tandem            | 2                |
| 58       | F   | R    | 52          | 84                | 72                         | /            | /        | AICA              | Loop              | 1                |
| 59       | F   | R    | 41          | 16                | 10                         | /            | /        | VA+AICA           | Tandem            | 3                |
| 60       | M   | R    | 44          | 84                | 60                         | /            | /        | AICA              | Loop              | 1                |
| 61       | F   | L    | 70          | 180               | 84                         | /            | √        | AICA              | Loop              | 1                |
| 62       | F   | L    | 52          | 36                | 30                         | /            | /        | AICA              | Arachnoid         | 2                |
| 63       | M   | L    | 50          | 96                | 72                         | /            | /        | AICA              | Loop              | 1                |
| 64       | F   | L    | 62          | 13                | 7                          | /            | /        | AICA              | Branch, Arachnoid | 3                |
| 65       | M   | R    | 47          | 24                | 21                         | √            | /        | AICA+PICA         | Sandwich          | 2                |
| 66       | F   | L    | 46          | 36                | 30                         | /            | /        | AICA              | Loop              | 1                |
| 67       | M   | R    | 68          | 48                | 46                         | √            | /        | PICA              | Loop              | 1                |
| 68       | F   | R    | 57          | 60                | 24                         | √            | /        | AICA              | Arachnoid         | 2                |
| 69       | M   | L    | 62          | 96                | 24                         | √            | /        | VA+AICA           | Tandem            | 3                |
| 70       | M   | L    | 63          | 84                | 60                         | /            | √        | AICA              | Loop              | 1                |
| 71       | F   | L    | 50          | 12                | 9                          | /            | /        | AICA              | Perforator        | 2                |
| 72       | F   | L    | 52          | 12                | 10                         | /            | /        | VA+AICA           | Tandem            | 3                |
| 73       | F   | L    | 52          | 120               | 72                         | /            | /        | AICA              | Loop              | 1                |
| 74       | M   | L    | 56          | 15                | 9                          | √            | /        | VA+AICA           | Tandem            | 3                |
| 75       | M   | L    | 54          | 13                | 4                          | √            | /        | VA+AICA           | Tandem            | 3                |
| 76       | F   | R    | 46          | 84                | 60                         | /            | /        | AICA              | Loop              | 1                |
| 77       | F   | R    | 40          | 132               | 60                         | /            | /        | AICA              | Loop              | 1                |
| 78       | F   | R    | 54          | 24                | 18                         | /            | √        | AICA+PICA         | Sandwich          | 2                |
| 79       | F   | L    | 36          | 12                | 10                         | /            | /        | PICA              | Perforator        | 2                |
| 80       | M   | R    | 58          | 12                | 11                         | √            | /        | AICA              | Tandem            | 2                |
| 81       | M   | R    | 60          | 120               | 72                         | /            | /        | AICA              | Loop              | 1                |
| 82       | M   | R    | 51          | 16                | 11                         | /            | /        | AICA+PICA         | Tandem            | 2                |
| 83       | F   | L    | 51          | 240               | 78                         | √            | /        | AICA              | Loop              | 1                |
| 84       | F   | R    | 63          | 84                | 60                         | /            | /        | AICA              | Loop              | 1                |
| 85       | F   | R    | 48          | 72                | 60                         | /            | /        | AICA              | Loop              | 1                |
| 86       | F   | L    | 57          | 36                | 10                         | /            | /        | VA+AICA           | Tandem            | 3                |
| 87       | F   | R    | 46          | 12                | 10                         | /            | /        | AICA+PICA         | Sandwich          | 2                |
| 88       | M   | L    | 59          | 6                 | 3                          | √            | /        | VA+AICA           | Tandem            | 3                |
| 89       | M   | R    | 49          | 6                 | 4                          | /            | /        | VA+AICA           | Tandem            | 3                |
| 90       | M   | L    | 75          | 120               | 96                         | /            | √        | AICA              | Loop              | 1                |
| 91       | F   | L    | 61          | 18                | 12                         | /            | √        | VA+AICA           | Tandem            | 3                |
| 92       | F   | R    | 39          | 6                 | 5                          | /            | /        | VA+AICA           | Tandem            | 3                |
| 93       | M   | R    | 65          | 240               | 72                         | /            | /        | AICA              | Loop              | 1                |
| 94       | F   | R    | 64          | 24                | 21                         | √            | /        | AICA              | Arachnoid         | 2                |
| 95       | F   | R    | 47          | 10                | 5                          | /            | /        | AICA              | Branch            | 2                |
| 96       | M   | L    | 62          | 180               | 60                         | √            | /        | AICA              | Loop              | 1                |

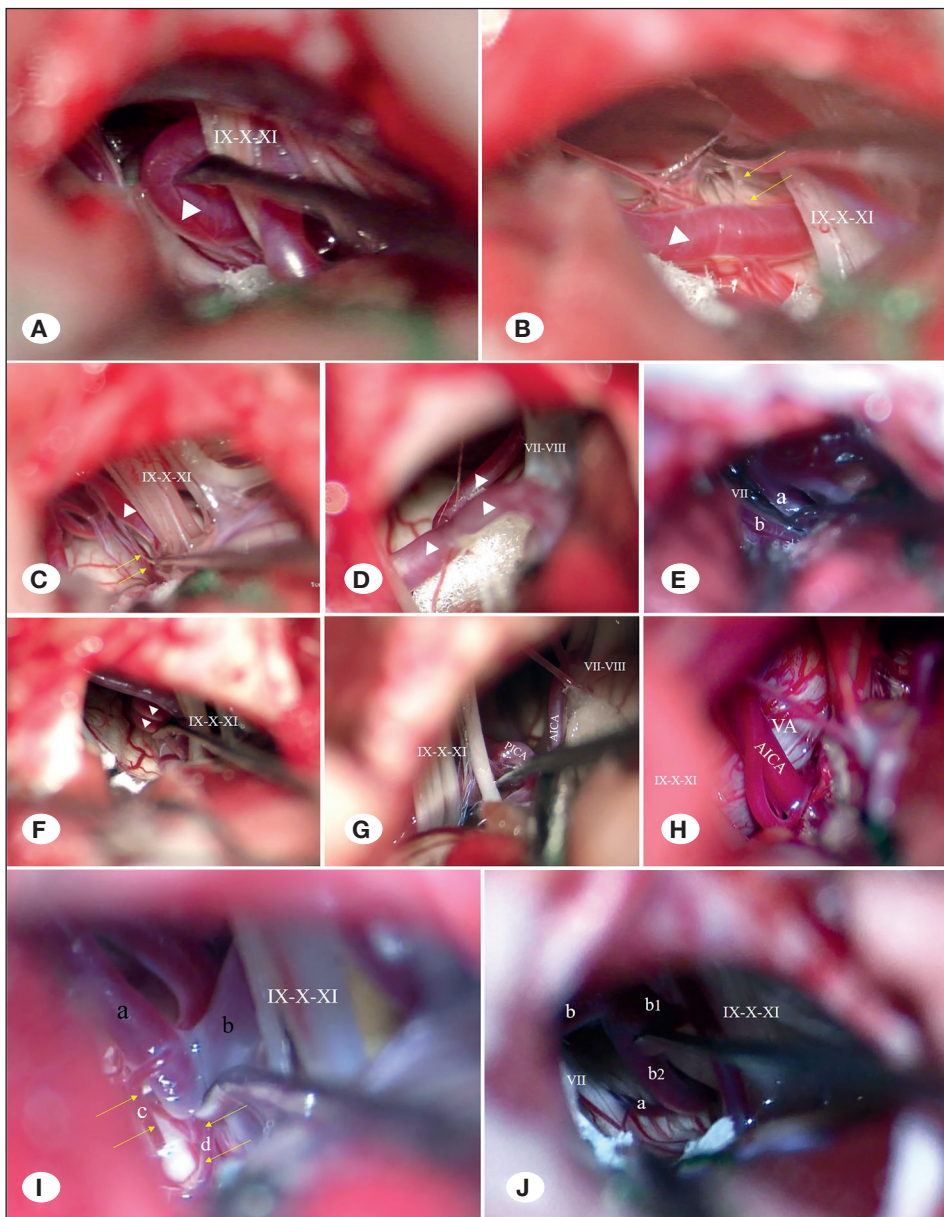
**M:** Male, **F:** Female, **L:** Left, **R:** Right, **AICA:** Anterior inferior cerebellar artery, **PICA:** Posterior inferior cerebellar artery, **VA:** Vertebral artery.



**Table II:** Influence of different vascular complexity levels on latency of spread

| Complexity Level | n  | Compression type         | Latency of spread (Mean ± SD) | F       | p-value |
|------------------|----|--------------------------|-------------------------------|---------|---------|
| Level 1          | 29 | Loop (n=29, 30.2%)       | 62.83 ± 16.00                 |         |         |
|                  |    | Arachnoid (n=6, 6.3%)    |                               |         |         |
|                  |    | Branch (n=6, 6.3%)       |                               |         |         |
| Level 2          | 33 | Perforator (n=7, 7.3%)   | 24.61 ± 15.02                 | 104.727 | <0.01   |
|                  |    | Sandwich (n=5, 5.2%)     |                               |         |         |
|                  |    | Tandem/no VA (n=9, 9.3%) |                               |         |         |
| Level 3          | 34 | Tandem/VA (n=29, 30.2%)  | 12.65 ± 11.42                 |         |         |
|                  |    | Mixed (n=5, 5.2%)        |                               |         |         |

**SD:** Standard deviation, **VA:** Vertebral artery.

**Figure 1: Samples of different types of responsible vessels.**

**A)** The loop type of patient No.30.  
**B)** The arachnoid type of patient No.43. Yellow arrow, thick arachnoid belt.  
**C)** The perforator type of patient No.40. Yellow arrow, perforating arteries from the offending vessel.  
**D)** The branch type of patient No.5.  
**E)** The sandwich type of patient No.49 formed by the offending vessels a and b.  
**F)** The tandem type of patient No.4 formed by the AICA.  
**G)** The tandem type of patient No.57 formed by AICA and PICA.  
**H)** The tandem type of patient No.88 formed by VA and AICA.  
**I)** The mixed type (arachnoid + perforator) is shown in patient No.11. The offending vessels a and b are closely bound by the arachnoid membrane. a, b, the offending vessels. c, d, perforating arteries from a and b.  
**J)** The mixed type (branch + sandwich) is shown in patient No.35. The facial nerve is clamped by vessels a and b. The vessel b is raised using a micro dissector and its branch vessels b1 and b2 are observed.  
**White triangle:** the responsible vessel. **AICA:** Anterior Inferior Cerebellar Artery. **PICA:** Posterior Inferior Cerebellar Artery. **VA:** Vertebral Artery.

**Table III:** Results of Multivariate Linear Regression Analysis

| Model            | Unstandardized Coefficients* |                | Standardized Coefficients* |         |              |
|------------------|------------------------------|----------------|----------------------------|---------|--------------|
|                  | B                            | Standard Error | Beta                       | t       | p-value      |
| (Constant)       | 81.059                       | 15.211         |                            | 5.329   | <b>0.000</b> |
| Sex              | -1.120                       | 3.421          | -0.021                     | -0.328  | 0.744        |
| Side             | -5.528                       | 3.359          | -0.109                     | -1.646  | 0.103        |
| Age              | 0.233                        | 0.190          | 0.091                      | 1.227   | 0.223        |
| Hypertension     | -0.573                       | 3.845          | -0.010                     | -0.149  | 0.882        |
| Diabetes         | 1.682                        | 5.055          | 0.023                      | 0.333   | 0.740        |
| Complexity level | -25.116                      | 2.064          | -0.807                     | -12.169 | <b>0.000</b> |

\*Dependent variable: Latency of spread.

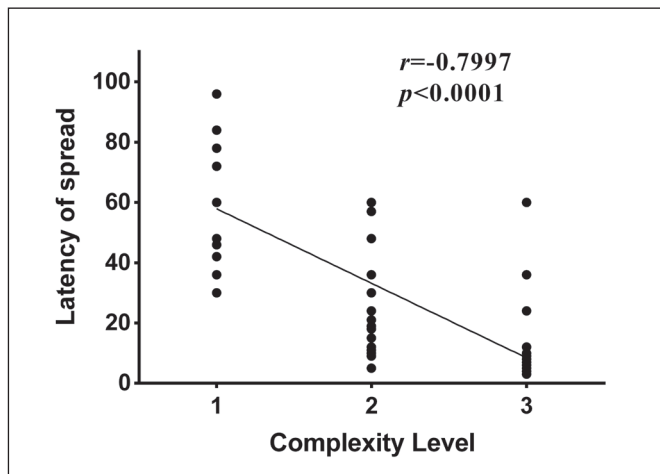


**Figure 2:** Spearman correlation analysis between vascular complexity level and the latency of spread. Spearman correlation analysis shows a strong negative correlation between vascular complexity level and the latency of spread ( $r = -0.7997$ ,  $p < 0.0001$ ).

hypertension, and diabetes, we also performed a multivariate linear regression analysis. As shown in Table III, the vascular complexity level was the main factor affecting the latency of spread ( $p < 0.01$ ), while the other factors had no significant effects.

**DISCUSSION**

Currently, there are few studies on the latency of spread and its significance remains unclear. Antonella Conte et al. described the definition of the latency of spread, the interval between the onset of eyelid spasm and subsequent involvement of the lower facial muscles (5). Disease duration refers to the total time from the first onset of the orbicularis oculi muscle to the patient’s visit (5,9,14,23). Since the duration is highly influenced by medical seeking willingness, the latency of spread may better reflect the characteristics of HFS progress. The core of MVD surgery is the proper treatment of the conflicting vessels to

relieve symptoms. To better describe the responsible vessels, we introduced six types of vascular classification (9,15). Further for better comparison and statistical analysis, we categorized the complexity of responsible vessels into three levels, combining the compression types and the difficulty of managing the responsible vessels. Level 1 refers to the loop type that is generally easy for the surgeon to handle. Level 3 included all the tandem types involving the vertebral artery. Due to the presence of the large vertebral artery, the surgical exposure was limited, and it was difficult for the surgeon to lift the vertebral artery and the vessels below it using a micro dissector. Five patients with mixed types were also classified as level 3 due to comparable surgical difficulty. The remaining compression types were defined as level 2. We believe that the difficulty of MVD indeed varies depending on the surgical techniques and operative experience of the surgeon. However, there should be no big difference in the view of the complexity of the offending vessels. Difficulties in handling responsible vessels include exposing and identifying them, decompressing them, and avoiding injury during surgery. In general, the lower complexity level means easier intraoperative exposure and identification of the offending vessels, simpler decompression procedures, and less possibility of injury to the brainstem, cranial nerves, and blood vessels. All the 96 patients were operated by the same surgeon, which effectively avoided the deviation caused by different surgeons.

One-way ANOVA showed significantly different latency of spread among three complexity levels. Spearman correlation analysis and multivariate linear regression analysis showed a significant negative correlation between vascular complexity level and the latency of spread. The pathogenesis of this result remains unknown. We hypothesize that it may be related to the compressive pressure and compressive area at the REZ of the facial nerve. Pei Zhang et al. directly measured the pressure values between the offending vessels and the facial nerve at the REZ intraoperatively using the Codman intracranial pressure Monitoring System. A positive correlation was determined between the severity of HFS symptoms and the pressure values (23). It is speculated that when the complexity level of offending vessels is level 2 or 3, the pressure of the

NVC may be high under the involvement of factors such as thick arachnoid belt, perforating arteries, branched vessels, and multiple vessels. However, the pressure theory may not fully explain this outcome. The symptomatic manifestation of a typical HFS is highly rigid; that is, it always progresses from the orbicularis oculi to the orbicularis oris muscle. The mechanism of this phenomenon has not been elucidated yet; however, it may be related to the stereo anatomy of facial nerve fibers. The nerve fibers that innervate the orbicularis oculi muscle are always affected first at the onset. Over time, under the influence of vascular pulsation and CSF flow, the compression of nerve fibers innervating the lower facial muscles follows. Thus, it is hypothesized that the higher the complexity level of offending vessels, the larger the compressive area at the REZ. The facial nerve fibers innervating the lower facial muscles are affected earlier, symptoms of patients progress faster, and corresponding latency of spread shortens.

Therefore, what are the clinical implications of our results? We think of it as a reminder to both doctors and patients, similar to the clinical significance of facial nerve MRI. Preoperative MRI can exclude secondary factors (13); however, it is only a reference and support for roughly predicting the offending vessels and compression types, which should not be viewed as diagnostic (6,17,19,20). Patients with apparent symptoms should be treated early as some of them may demonstrate facial nerve structural damage (14), which may lead to unsatisfactory remission after surgery (2). If symptoms develop from the eyelid to the lower muscles quickly, the offending vessels may be complicated. Patients are encouraged to accept MVD as soon as possible, and surgeons should be alert to potentially intractable vascular conditions during surgery.

## CONCLUSION

As an important clinical indicator, the latency of spread can reflect the complexity level of offending vessels in patients with typical HFS before MVD.

## ACKNOWLEDGEMENTS

We thank all the patients with typical HFS who participated in the study.

### AUTHORSHIP CONTRIBUTION

Study conception and design: XW, BC

Data collection: XW

Analysis and interpretation of results: XW, BC, SL

Draft manuscript preparation: XW

Critical revision of the article: BC, SL

Other (study supervision, fundings, materials, etc.): SL

All authors (XW, BC, SL) reviewed the results and approved the final version of the manuscript.

## REFERENCES

- Amagasaki K, Watanabe S, Naemura K, Nakaguchi H: Microvascular decompression for hemifacial spasm: How can we protect auditory function? *Br J Neurosurg* 29:347-352, 2015. <https://doi.org/10.3109/02688697.2014.1003033>
- Baldauf J, Rosenstengel C, Schroeder HWS: Nerve compression syndromes in the posterior cranial fossa. *Dtsch Arztebl Int* 116:54-60, 2019. <https://doi.org/10.3238/arztebl.2019.0054>
- Barker FG 2nd, Jannetta PJ, Bissonette DJ, Shields PT, Larkins MV, Jho HD: Microvascular decompression for hemifacial spasm. *J Neurosurg* 82:201-210, 1995. <https://doi.org/10.3171/jns.1995.82.2.0201>
- Campos-Benitez M, Kaufmann AM: Neurovascular compression findings in hemifacial spasm. *J Neurosurg* 109:416-420, 2008. <https://doi.org/10.3171/JNS/2008/109/9/0416>
- Conte A, Falla M, Diana MC, Bologna M, Suppa A, Fabbrini A, Colosimo C, Berardelli A, Fabbrini G: Spread of muscle spasms in hemifacial spasm. *Mov Disord Clin Pract* 2:53-55, 2015. <https://doi.org/10.1002/mdc3.12106>
- El Refaee E, Langner S, Baldauf J, Matthes M, Kirsch M, Schroeder HW: Value of 3-dimensional high-resolution magnetic resonance imaging in detecting the offending vessel in hemifacial spasm: Comparison with intraoperative high definition endoscopic visualization. *Neurosurgery* 73:58-67; discussion 67, 2013. <https://doi.org/10.1227/01.neu.0000429838.38342.e2>
- Green KE, Rastall D, Eggenberger E: Treatment of blepharospasm/hemifacial spasm. *Curr Treat Options Neurol* 19:41, 2017. <https://doi.org/10.1007/s11940-017-0475-0>
- Hitotsumatsu T, Matsushima T, Inoue T: Microvascular decompression for treatment of trigeminal neuralgia, hemifacial spasm, and glossopharyngeal neuralgia: Three surgical approach variations: Technical note. *Neurosurgery* 53:1436-1441; discussion 1442-1433, 2003. <https://doi.org/10.1227/01.NEU.0000093431.43456.3B>
- Lee JA, Kong DS, Lee S, Park SK, Park K: Clinical outcome after microvascular decompression according to the progression rates of hemifacial spasm. *World Neurosurg* 134:e985-e990, 2020. <https://doi.org/10.1016/j.wneu.2019.11.052>
- Lee JM, Park HR, Choi YD, Kim SM, Jeon B, Kim HJ, Kim DG, Paek SH: Delayed facial palsy after microvascular decompression for hemifacial spasm: Friend or foe? *J Neurosurg* 129:299-307, 2018. <https://doi.org/10.3171/2017.3.JNS162869>
- Lee S, Park SK, Lee JA, Joo BE, Kong DS, Seo DW, Park K: A new method for monitoring abnormal muscle response in hemifacial spasm: A prospective study. *Clin Neurophysiol* 129:1490-1495, 2018. <https://doi.org/10.1016/j.clinph.2018.03.006>
- Lefaucheur JP: New insights into the pathophysiology of primary hemifacial spasm. *Neurochirurgie* 64:87-93, 2018. <https://doi.org/10.1016/j.neuchi.2017.12.004>
- Liu J, Yuan Y, Fang Y, Zhang L, Xu XL, Liu HJ, Zhang Z, Yu YB: Microvascular decompression for atypical hemifacial spasm: Lessons learned from a retrospective study of 12 cases. *J Neurosurg* 124:397-402, 2016. <https://doi.org/10.3171/2015.3.JNS142501>



14. Na BS, Cho JW, Park K, Kwon S, Kim YS, Kim JS, Youn J: Severe hemifacial spasm is a predictor of severe indentation and facial palsy after microdecompression surgery. *J Clin Neurol* 14:303-309, 2018. <https://doi.org/10.3988/jcn.2018.14.3.303>
15. Park JS, Kong DS, Lee JA, Park K: Hemifacial spasm: Neurovascular compressive patterns and surgical significance. *Acta Neurochir (Wien)* 150:235-241; discussion 241, 2008. <https://doi.org/10.1007/s00701-007-1457-x>
16. Rosenstengel C, Matthes M, Baldauf J, Fleck S, Schroeder H: Hemifacial spasm: Conservative and surgical treatment options. *Dtsch Arztebl Int* 109:667-673, 2012. <https://doi.org/10.3238/arztebl.2012.0667>
17. Sekula RF, Jr., Frederickson AM, Branstetter Bft, Oskin JE, Stevens DR, Zwagerman NT, Grandhi R, Hughes MA: Thin-slice T2 MRI imaging predicts vascular pathology in hemifacial spasm: A case-control study. *Mov Disord* 29:1299-1303, 2014. <https://doi.org/10.1002/mds.25947>
18. Son BC, Ko HC, Choi JG: Intraoperative monitoring of Z-L response (ZLR) and abnormal muscle response (AMR) during microvascular decompression for hemifacial spasm. Interpreting the role of ZLR. *Acta Neurochir (Wien)* 160:963-970, 2018. <https://doi.org/10.1007/s00701-017-3462-z>
19. Wang A, Jankovic J: Hemifacial spasm: Clinical findings and treatment. *Muscle Nerve* 21:1740-1747, 1998. [https://doi.org/10.1002/\(SICI\)1097-4598\(199812\)21:12<1740::AID-MUS17>3.0.CO;2-V](https://doi.org/10.1002/(SICI)1097-4598(199812)21:12<1740::AID-MUS17>3.0.CO;2-V)
20. Yaltho TC, Jankovic J: The many faces of hemifacial spasm: Differential diagnosis of unilateral facial spasms. *Mov Disord* 26:1582-1592, 2011. <https://doi.org/10.1002/mds.23692>
21. Yang M, Zheng X, Ying T, Zhu J, Zhang W, Yang X, Li S: Combined intraoperative monitoring of abnormal muscle response and Z-L response for hemifacial spasm with tandem compression type. *Acta Neurochir (Wien)* 156:1161-1166; discussion 1166, 2014. <https://doi.org/10.1007/s00701-014-2015-y>
22. Zhang KW, Shun ZT: Microvascular decompression by the retrosigmoid approach for idiopathic hemifacial spasm: Experience with 300 cases. *Ann Otol Rhinol Laryngol* 104:610-612, 1995. <https://doi.org/10.1177/000348949510400804>
23. Zhang P, Selim MH, Wang H, Kuang W, Wu M, Ji C, Hu G, Wu L, Zhu X, Guo H: Intraoperative measuring of the offending vessel's pressure on the facial nerve at root exit zone in patients with hemifacial spasm during microvascular decompression: A prospective study. *World Neurosurg* 122:e89-e95, 2019. <https://doi.org/10.1016/j.wneu.2018.09.080>
24. Zhang X, Zhao H, Tang YD, Zhu J, Zhou P, Yuan Y, Li ST: The effects of combined intraoperative monitoring of abnormal muscle response and z-l response for hemifacial spasm. *World Neurosurg* 108:367-373, 2017. <https://doi.org/10.1016/j.wneu.2017.08.160>
25. Zheng X, Hong W, Tang Y, Wu Z, Shang M, Zhang W, Zhong J, Li S: Sympathetic nerves bridge the cross-transmission in hemifacial spasm. *Neurosci Lett* 517:52-55, 2012. <https://doi.org/10.1016/j.neulet.2012.04.023>
26. Zheng X, Hong W, Tang Y, Ying T, Wu Z, Shang M, Feng B, Zhang W, Hua X, Zhong J, Li S: Discovery of a new waveform for intraoperative monitoring of hemifacial spasms. *Acta Neurochir (Wien)* 154:799-805, 2012. <https://doi.org/10.1007/s00701-012-1304-6>